



## Wall conditioning technique development in Tore Supra with permanent magnetic field by ICRF wave injection

E. Gauthier<sup>\*</sup>, E. de la Cal, B. Beaumont, A. Becoulet, C. Gil, C. Grisolia, A. Grosman, T. Hutter, H. Kuus, L. Ladurelle, J.L. Segui

*Association Euratom-CEA sur la fusion contrôlée, CEA Cadarache, F-13108 St. Paul-les-Durance Cedex, France*

### Abstract

Wall conditioning techniques tokamaks with a permanent magnetic field have been performed in Tore Supra by using an ion cyclotron range frequency (ICRF) facility. Plasmas have been produced by injection of ICRF power in the range from 40 kW to 350 kW either in helium or deuterium gas. Electron density in the range of  $1 \cdot 10^{17}$  to  $6 \cdot 10^{17} \text{ m}^{-3}$  and electron temperatures from 1.5 to 8 eV have been measured depending on the gas pressure and injected power. Energetic neutral atoms of hydrogen and deuterium with energies up to 50 keV have been produced. High hydrogen removal rates have been obtained in helium discharges, either in a continuous or pulsed operation mode.

*Keywords:* Wall conditioning; ICRF; Tore Supra

### 1. Introduction

Conditioning techniques are extensively used in most of the tokamaks and have significantly improved the plasma performance in recent years [1–4]. High performance shots performed in large present-day tokamaks, such as the Hot Ion mode in JET, Very High mode in DIII-D or Supershot in TFTR, require a low recycling regime which is obtained by using intensive conditioning techniques such as boronization, helium glow discharges, repetitive helium shots or beryllium evaporation. Moreover, in addition to decreasing the low Z impurity content, such as oxygen, these techniques tend to improve the pumping capability of the wall in a transient way. Even though ITER will not be operated in such modes, conditioning will be probably required between shots to minimise the tritium inventory in the wall and to obtain reproducible and optimised conditions for the subsequent discharge start-up [5]. Due to the permanent toroidal magnetic field in ITER, helium glow discharges cannot be operated between shots. Pulsed helium discharge, even at a lower current than the nominal

value, would probably not be possible to run for long periods due to excessive heat deposition in the toroidal cryogenic system.

Systematic beryllium evaporation would build up a continually increasing layer of beryllium mixed with wall material and hydrogen isotopes, producing an unacceptable level of tritium trapped in the wall. In summary, none of the conditioning techniques presently used in tokamak is applicable to ITER, since the toroidal magnetic field will always be present.

Tore Supra, being a large tokamak with a permanent and high toroidal magnetic field (4.5 T), is then very adequate to investigate alternative conditioning techniques that are relevant to ITER.

In this paper we report the results of a conditioning technique performed on Tore Supra by using the Ion Cyclotron Range of Frequency (ICRF) facility.

The theory of plasma production in a tokamak using rf power in the ion cyclotron range of frequency has been investigated by many authors [6–9]. First experimental results were reported from Textor using hydrogen and deuterium plasma [10,11], in order to obtain an initial rf preionisation of neutral gas to save volt-seconds in a tokamak discharge. In this paper, we investigated the main parameters of plasma produced by ICRF wave injection

<sup>\*</sup> Corresponding author.

and the conditioning efficiency as function of the ICRF input power measured at the generator, total pressure, fuelling gas and discharge duration.

## 2. Experimental set-up

Radio frequency plasmas have been produced by using ICRF wave injection. Two antennae, located at an angle of 180 degrees to each other in a toroidal direction, have been operated alternately. The chosen frequency was 48 MHz and the toroidal magnetic field was kept constant at 3.8 T, on the axis. With such parameters, neither deuterium nor helium, which have been used as fuelling gas, have a resonance absorption layer for the first harmonic inside the vacuum vessel.

The ion cyclotron frequency  $\omega$  is

$$\omega = qB/m, \quad (1)$$

where  $B$  is the magnetic field,  $q$  the ion charge and  $m$  the ion mass. Since the plasma we produce has a low ionisation ratio, only the ions with charge equal to one are taken into account and multicharged ions are considered as negligible (as it is usually the case in low temperature plasma). The hydrogen absorption layer for the first harmonic, as well as deuterium for the 2nd harmonic are located at a major radius of 2.8 m, the antennae being positioned between 3 and 3.1 m and the inner wall at 1.56 m. The poloidal and toroidal plasma symmetry has been characterised by using a visible spectrometer looking along different chords in a poloidal cross section CCD looking different toroidal directions.

Plasma densities were measured with an interferometer giving 5 vertical line integrated densities.

Two effects govern the conditioning efficiency: first, the outgassing rate of the impurities from the wall and secondly the ionisation rate of the desorbed molecules which induce a redeposition process instead of having the impurities evacuated through the pumps. At low temperature (less than 10 eV), electron temperature is the main parameter which determines the hydrogen ionisation rate (at a given electron density). The electron temperature was measured by using two different methods: (a) Electron cyclotron emission and (b) from the ratio of two helium lines at 728 and 706 nm, as described by Pospieszczyk et al. [12], although the values lied in the low electron temperature measurement limits, which is about some electron-volts.

The total pressure was measured with capacitance and ion gauges and partial pressures either with a differentially pumped mass spectrometer or a Penning gauge coupled with optical detection [13] and calibrated for hydrogen partial pressure measurements from  $5 \cdot 10^{-4}$  to 1 Pa. Both instruments were located in the pumping duct. The deuterium partial pressure for a high level of helium in the gas

was determined by using a technique described elsewhere [14].

The vacuum vessel, with a  $50 \text{ m}^3$  volume, was pumped with 3 turbomolecular pumps providing a pumping speed of  $8 \text{ m}^3/\text{s}$  for helium and deuterium.

## 3. Results

To determine the breakdown conditions, 20 ms ICRF pulses every 10 s were performed with a slowly increasing level of gas injection. Above a threshold input power of 30 kW, a narrow pressure window was found around  $10^{-1}$  Pa in deuterium and  $1.5 \cdot 10^{-1}$  Pa in helium. This window is

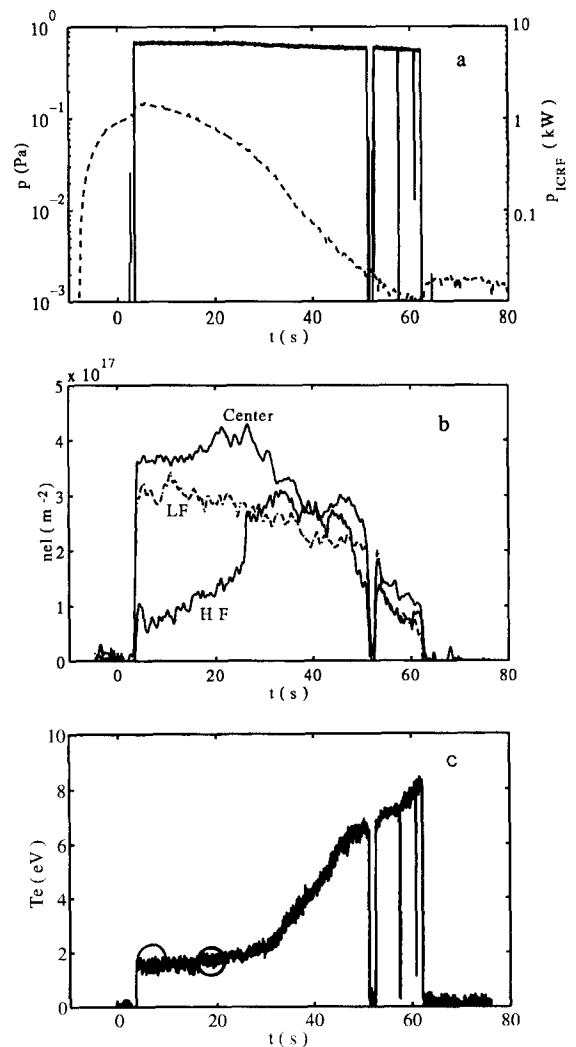


Fig. 1. (a) ICRF injected power (—) and helium pressure (---), (b) line integrated densities: high field (HF), central and low field (LF) (c) electron temperature (ECE line, He726/706: circle) as function of time.

probably related to the minimum in the Paschen curve of the breakdown voltage as function of the pressure but has not been investigated yet. Once the plasma has been generated, the discharge is stable over a wide pressure range. Fig. 1 shows the variation of the line integrated electron density during a helium discharge where the pressure decreases from  $2 \cdot 10^{-1}$  Pa to less than  $10^{-3}$  Pa (Fig. 1a). At high pressure, the poloidal asymmetry is high and the plasma is mainly localised on an outer radius, this asymmetry decreases with the pressure (Fig. 1b), from  $10^{-1}$  to  $10^{-2}$  Pa, the density profile being almost flat. Spectroscopic measurements of the helium line at 706 nm, on inner and outer chords in a poloidal cross section show the same poloidal asymmetry behaviour as function of the pressure. A further pressure reduction induces a decrease of the plasma density, while the electron temperature measured with ECE radiometry (Fig. 1c) increases from 1.5 eV to 8 eV (in the  $10^{-2}$  to  $10^{-3}$  Pa range). The helium singlet–triplet line intensity ratio was measured for the high pressure conditions ( $10^{-1}$  Pa); although in the lower measurement limit, an electron temperature of about 2 eV was extrapolated, in good agreement with the ECE data. Toroidal asymmetries have been investigated by using alternately two ICRF antennae. Although one antenna is close to the interferometer, the line averaged density, normalised to the input power is similar in both cases and the images obtained with the tangential view of the CCD camera confirm this homogeneity on the toroidal direction. ICRF power was increased stepwise from 20 to 340 kW; Fig. 2 shows the average electron density evolution as function of ICRF power in a helium discharge at a pressure of  $10^{-1}$  Pa. High injected power generates asymmet-

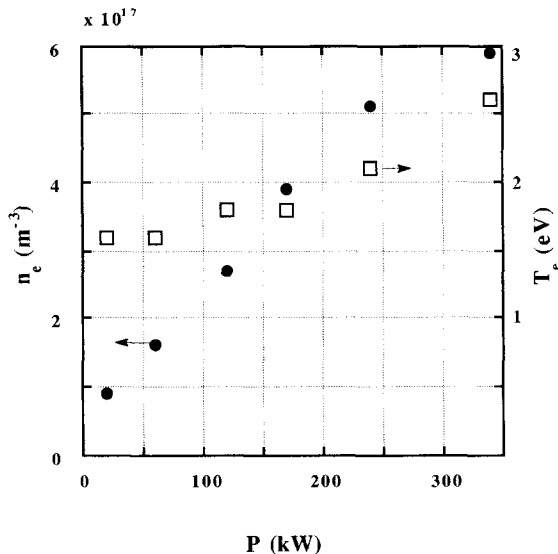


Fig. 2. Average electron density (●) and electron temperature (□) in helium conditioning discharge as function of ICRF power ( $p \approx 10^{-1}$  Pa).

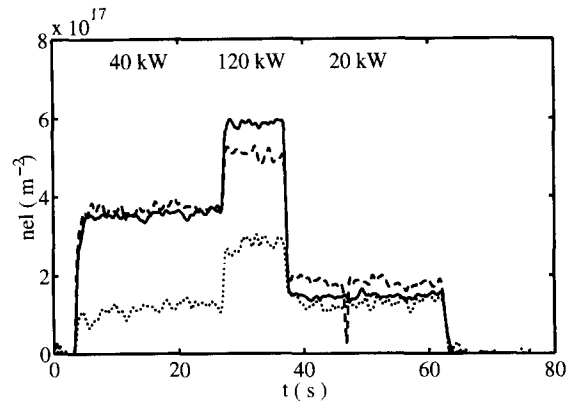


Fig. 3. Line integrated densities at the inner (···), outer (—), central line (---) and ICRF power as function of time.

ric density profiles by preferentially increasing the density on the outer part as deduced either from the tangential CCD camera showing light emission localised on the outer side and from the interferometer showing, as we can see on Fig. 3, a large density increase in the outer and central chords when the ICRF power is increased from 20 to 40 and 120 kW. It can be observed that the additional injected power increases the plasma density at a constant electron temperature of about 2 eV. To understand this behaviour we have to keep in mind that the ionisation fraction, even at high density, is very low. In such plasmas, the ratio  $n_e/n_a$ , where  $n_e$  is the ion density and  $n_a$  is the density of the neutrals, is about  $10^{-2}$ . This experimental data are in very good agreement with the simulations performed by Lysoivan [9] showing that in a plasma generated by ICRF waves injection, the density increases at an electron temperature of about 3 eV until the ratio  $n_e/n_a$  is unity, after which, the density stays constant and the electron temperature starts to increase to a value depending on the input power. In fact, both experiments where the power density per atom has been increased, either by decreasing the pressure at constant ICRF power (Fig. 1) or by increasing the injected power at constant pressure (Fig. 2), show that the electron temperature start to increase with the power density when the ratio  $n_e/n_a$  is about 10%. Below this value, increasing the power density per atom increases the electron density at constant electron temperature.

Since ICRF helium discharges are produced to desorb large amounts of hydrogen isotopes, we have to take into account the neutral and ion densities of not only helium but also of hydrogen and deuterium desorbed from wall. Their partial pressures, detected by mass spectrometry and a Penning gauge coupled with optical detection, are typically a few percent during the experiments, although this depends strongly on the first wall surface concentration. The neutral species will be ionised by electron collision with a characteristic time  $\tau_i$  and will be heated, with their

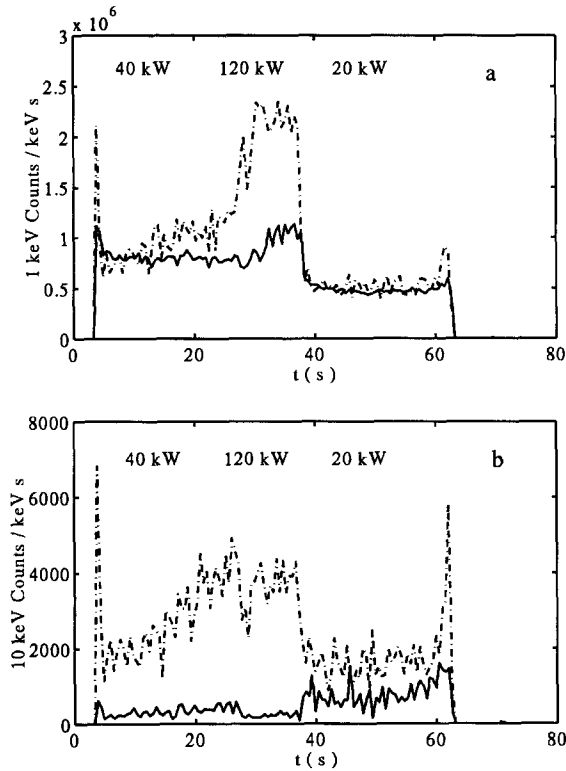


Fig. 4. Charge exchange neutrals flux of hydrogen (—) and deuterium (---) at 1 keV (a) and 10 keV (b) as a function of time for three level of ICRF power.

corresponding heating efficiency, by the injected ICRF power. As described in more detail elsewhere [15], the ion electron collision frequency  $\omega_{ei}$  does not satisfy the condition for thermal equilibrium between the electrons and the different ions species,  $\omega_{ei} \gg \omega_E$ ,  $\omega_E$  being the energy loss frequency, which is limited by CX reactions. Therefore, each ion species has a characteristic ion energy distribution, as obtained with the H and D energetic CX analyser (He CX were not measured). At high pressures ( $10^{-1}$ – $10^{-2}$  Pa), the energy distributions are Maxwellian, with hydrogen and deuterium ion temperatures about 1 keV. Increasing the injected power, increases the number of counts in the detector but does not change the ion temperature (Fig. 4). At low pressure ( $< 10^{-2}$  Pa), a suprathermal energy tail appears principally in the hydrogen distribution, 50 keV CX neutrals being measured.

#### 4. Discussion

To characterise the conditioning efficiency in the ICRF helium discharge and to compare it with other techniques, we took the hydrogen and deuterium pumped flux,  $Q_p$ , as a criterion. Since deuterium is the fuelling gas for normal plasma operation, deuterium compounds (HD,  $D_2$ ) domi-

nate the outgassing of hydrogenic molecules, as deduced from mass spectrometer measurements [16]. In the following discussion, hydrogen will be used as a generic term covering the three hydrogenic compounds:  $H_2$ , HD and  $D_2$ . Fig. 5 shows the hydrogen pressure during and after ICRF conditioning discharge for two different modes of operation: a continuous regime at low input power and low electron density and a pulsed regime with higher input power and density. The electron density plotted on the same curve indicates when the discharge is switched on and off. An important result is the high hydrogen pressure which provides a removal rate of about  $100 \text{ Pa} \cdot \text{m}^3/\text{h}$  with a maximum value of  $260 \text{ Pa} \cdot \text{m}^3/\text{h}$  at the very beginning of the conditioning process. In such a plasma, the hydrogen ionisation time constant  $\tau_i = 1/n_e \langle \sigma v \rangle$ , where  $n_e$  is the electron density and  $\langle \sigma v \rangle$  is the electron ionisation rate, is about one order of magnitude lower than the hydrogen molecules residence time constant  $\tau_s = V/S$ , where  $V$  is the vacuum volume and  $S$  the hydrogen pumping speed. It was anticipated that the conditioning efficiency of a continuous discharge may be very low due to a short ionisation length and a high redeposition ratio of desorbed molecules. The hydrogen pressure, averaged over two minutes, is plotted on Fig. 6, as function of ICRF power, arrows showing the time evolution during experi-

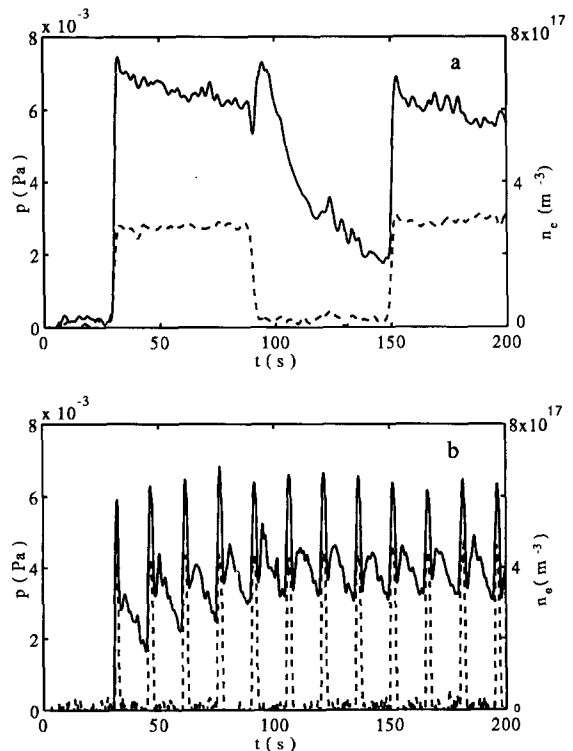


Fig. 5. Electron density (---) and hydrogen pressure (—) as function of time for a continuous (a) and a pulsed mode helium discharge (b).

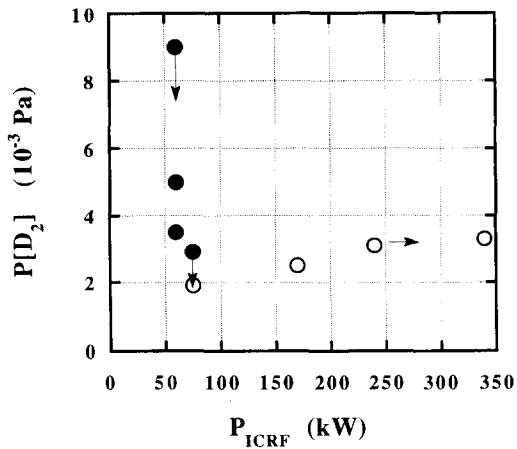


Fig. 6. Hydrogen pressure as function of ICRF power for pulsed (○) and continuous mode (●). Arrows indicate time evolution during the experiments.

ments from the first to the last conditioning discharge. In fact, the average hydrogen pressure, shown in Fig. 6, is similar in continuous and pulsed modes (except the first point which is an initial and transient value).

During the discharge, the hydrogen desorption rate from the wall  $Q_w$  is equal to

$$Q_w = P \cdot S + V dP/dt + f \cdot Q_w, \quad (2)$$

where  $P$  is the hydrogen partial pressure and  $f$  the hydrogen reionisation probability defined as

$$f \cong \tau_i^{-1} / (\tau_s^{-1} + \tau_i^{-1}). \quad (3)$$

In a steady state regime, the pumped flux  $Q_p$  is

$$Q_p = P \cdot S = (1 - f) Q_w. \quad (4)$$

Assuming that the hydrogen ion redeposits into the wall with a sticking coefficient equal to one,  $(1-f)$  is the outpumping probability.

From the hydrogen pressure, we can therefore deduce the hydrogen outgassing rate from the wall for a given electron density and temperature. At an hydrogen pressure of  $3 \cdot 10^{-3}$  Pa (average value in Fig. 6) with an electron density of  $3 \cdot 10^{17} \text{ m}^{-3}$  and an electron temperature of 1.5 eV, providing an hydrogen ionisation time of 2 s and a redeposition probability of 75%, the outgassing rate is about  $6 \cdot 10^{13} \text{ H/cm}^2\text{s}$ . At higher ICRF injected power, this rate grows up to  $9 \cdot 10^{14} \text{ H/cm}^2\text{s}$  when the electron density and electron temperature increase to  $6 \cdot 10^{17} \text{ m}^{-3}$  and 2.5 eV, while redeposition increases to 88.5%. However, since the hydrogen ionisation rate is strongly dependant on electron temperature around 2 eV [17], an uncertainty of 1 eV on the measured electron temperature would induce a variation of one order of magnitude in the calculated outgassing rate. Therefore, the minimum value can be simply evaluated from the measured pumped hydrogen flux, about  $1.5 \cdot 10^{13} \text{ H/cm}^2\text{s}$  for a hydrogen pressure of

$3 \cdot 10^{-3}$  Pa and the maximum value could be equal to  $10^{16} \text{ H/cm}^2\text{s}$  at the highest electron density and temperature.

In summary, ICRF conditioning discharge in helium can be operated either in a continuous mode with a lower outgassing rate and higher pumping probability or in pulsed mode with higher outgassing rate and lower pumping probability with approximately the same global efficiency. Therefore, the conditioning efficiency could be increased by controlling separately the electron density and the electron temperature in the ICRF discharge to minimise the hydrogen redeposition probability.

The high hydrogen removal rates, achieved in these experiments, are one order of magnitude higher than those obtained in a helium glow discharge at a cathode current density of  $3 \mu\text{A/cm}^2$ . This would allow the recovery of the total injected gas for a plasma discharge, typically  $10 \text{ Pa m}^3$  in Tore Supra, within approximately 10 min of conditioning with helium ICRF discharge. This has been confirmed by the particle balance analysis performed for two similar ICRF deuterium discharges, Fig. 7, showing a wall pumping capability enhancement of  $25 \text{ Pa m}^3$  after 30 min of conditioning.

The high conditioning efficiency obtained in our experiments can be partly explained by the intense ion flux bombarding the walls. We can compare the primary ion flux to the wall in such discharge and, for instance, in a glow discharge. Electron density and temperature measurements performed with Langmuir probes on typical GDC give values of about  $10^{12} \text{ m}^{-3}$  and 2 eV [18]. For a similar temperature, the electron density in ICRF discharges is about  $10^{17} \text{ m}^{-3}$  and consequently the ion flux to the wall is 5 orders of magnitude higher. Of course, the ionisation time constant for hydrogen is not comparable and we can assume that 100% of desorbed molecules are evacuated through the pump during GDC whereas it is about 25% or less in an ICRF discharge, as it has been shown previously.

Hydrogen desorption also occurs induced by the energetic CX neutrals bombarding the wall. This contribution

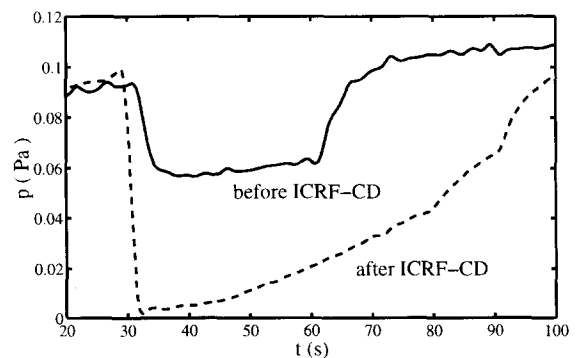


Fig. 7. Deuterium pressure as function of time for two similar discharges performed before (—) and after (---) ICRF conditioning.

is negligible in GDC but is very important in an ICRF discharge due to the high densities of ions and neutrals. The charge exchange spectrum of hydrogen and deuterium, in helium discharges at  $10^{-1}$  Pa, can both be fitted by a Maxwellian distribution with a temperature of 1 keV. The charge exchange cross section for the reaction:  $H^+ + He \rightarrow H + He^+$  at this temperature and pressure gives a confinement time for hydrogen ion of about 1 ms [19], inducing an energetic neutral flux impinging to the wall of  $10^{16}$  H/cm<sup>2</sup>s. This flux is about one order of magnitude higher than the ion flux, for the parameters given previously,  $n_e = 10^{17}$  m<sup>-3</sup>,  $T_e = 2$  eV. In which extent each of these fluxes contribute to the outgassing process, need still to be investigated. When the helium pressure decreases, less collisions occur and both hydrogen and deuterium suprathermal ions are created as deduced from the charge exchange spectrum, showing atoms with energy up to 50 keV. TRIM code simulations [20] give a mean range of penetration of about 0.5  $\mu$ m for such particles in carbon. This behaviour shows a great potential in a tokamak such ITER to permit conditioning of deep saturated layers and tritium removal by isotope change over.

Development of a new antenna, allowing to couple energy directly to the helium ions at the resonance frequency, is planned. Optimisation of this conditioning technique, based on results of these experiments and those performed on Textor [21] will be investigated on both tokamaks.

## 5. Conclusion

Conditioning of Tore Supra by using ICRF power injection in a permanent magnetic field of 3.8 T has been studied and its efficiency has been demonstrated. Plasmas have been generated either in deuterium or helium in a wide range of pressure and ICRF power. Electron temperature and density are controlled by the ratio of injected power over pressure. High flux of energetic particles up to 50 keV have been measured. Conditioning with helium ICRF discharges produces high hydrogen desorption rate

either in continuous or pulsed discharges. During these first experiments, a maximum hydrogen removal rate of 260 Pa m<sup>3</sup> h<sup>-1</sup> has been obtained as initial value and an average of 50 Pa m<sup>3</sup> h<sup>-1</sup> on a long time basis. The potential application of this technique to ITER is now demonstrated and need to be optimised.

## Acknowledgements

The authors acknowledge J.Y. Pascal and S. Vartanian for their technical support during the experiments.

## References

- [1] J. Winter, J. Nucl. Mater. 145–147 (1986) 131.
- [2] J. Winter and H.G. Esser, J. Nucl. Mater. 162–164 (1989) 713.
- [3] J. Orchard, A.T. Peacock and G. Saibene, J. Nucl. Mater. 200 (1993) 395.
- [4] G.L. Jackson et al., J. Nucl. Mater. 196–198 (1992) 236.
- [5] H. Nakamura, J. Dietz and P. Ladd, Fusion Technol. 28 (1995) 705.
- [6] A.I. Lyssoivan et al., Nucl. Fusion 32(8) (1992) 1361.
- [7] K. Wong et al., Rev. Sci. Instr. 53 (1982) 409.
- [8] N.I. Nazarov et al., 13th EPS Conf., Schliersee (1986) p. 303.
- [9] M.D. Carter et al., Nucl. Fus. 30(4) (1990) 723.
- [10] A.I. Lyssoivan et al., 22th EPS Conf., Bournemouth, Vol. 19C, Part III (1995) p. 341.
- [11] J. Winter, private communication, Cadarache, Oct. (1994).
- [12] A. Pospieszczyk et al., UCLA-PPG-1402 (1991).
- [13] A. Hardtke, thesis, Jül-2269 (1989).
- [14] E. Gauthier, 22th EPS Conf., Bournemouth, Vol. 19C, Part I (1995) p. 413.
- [15] E. de la Cal and E. Gauthier, Plasma Phys. Controlled Fusion, to be published.
- [16] E. de la Cal and E. Gauthier, J. Vac. Sci. Technol., submitted.
- [17] R.L. Freeman and E.M. Jones, CLM-R 137 (1974).
- [18] G. Saibene et al., J. Nucl. Mater. 220–222 (1995) 617.
- [19] R. Hoekstra et al., Suppl. Nucl. Fusion 3 (1992) 630.
- [20] J. Biersack and W. Eckstein, Appl. Phys. 34 (1984) 73.
- [21] H.G. Esser, these Proceedings, p. 861.